Progress In Electromagnetics Research B, Vol. 18, 101–119, 2009

BLIND JOINT DOA AND DOD ESTIMATION AND IDENTIFIABILITY RESULTS FOR MIMO RADAR WITH DIFFERENT TRANSMIT/RECEIVE ARRAY MANIFOLDS

X. Zhang, X. Gao, G. Feng, and D. Xu

Department of Electronic Engineering
Nanjing University of Aeronautics & Astronautics
Nanjing 210016, China

Abstract—This paper derives its link of direction of arrival (DOA) and direction of departure (DOD) estimation problem for multi-input multi-output (MIMO) radar to the trilinear model. With the exploitation of this link, we present a trilinear decomposition-based blind algorithm for angle estimation in MIMO radar. After the algorithmic presentation and discussions for identifiability results, trilinear decomposition-based angle estimation under different array conditions has also been investigated. Our proposed algorithm works well without either spectral peak searching or pair matching, has better angle estimation performance than ESPRIT, and even supports small sampling sizes. Simulation trials testify that the merits of our algorithmic performance are in collaboration with theoretical findings.

1. INTRODUCTION

Well-established by the original concept of multi-input multi-output (MIMO) radar, which takes advantage of multiple antennas to simultaneously transmit diverse waveforms that could be freely chosen and utilizes multiple antennas to receive the reflected signals, many potential benefits have been demonstrated over a conventional phased-array radar, see [1–4] and references therein. To the best of our knowledge, compared with other systems with a single transmit antenna, MIMO radar systems have additional degrees of freedom that can overcome fading effect, enhance space resolution, strengthen parameter identifiability and improve target detection performance [5–9]. Direction of arrival (DOA) and direction of departure (DOD)

Corresponding author: X. Zhang (fei_zxf@163.com).

estimation algorithms for MIMO radar have been investigated in [10–12]. [10, 12] have discussed the ESPRIT algorithm which exploited the invariance property of both the transmit array and the receive array for direction estimation in MIMO radar systems, while [11] presented another ESPRIT algorithm without pairing, whose complexity was lower than [10]; nevertheless, both of them have almost the same angle estimation performance. Notably, most relevant works have been on the basis of transmit/receive uniform linear arrays (ULA). In this paper, blind joint DOA and DOD estimation for MIMO radar with different transmit/receive array manifolds is investigated in this paper.

ESPRIT is a certain technique of closed-form eigen structure-based parameter estimation that requires the data to possess certain "invariance" structures. In the past decades, ESPRIT-based ideas have revolutionized sensor array signal processing. Interestingly, a general principle underlying ESPRIT has flourished other scientific fields and disciplines independently. As commonly referred in a number of ways, the principle includes trilinear model or trilinear decomposition. It is well known that most of signal processing methods are based on the theory of matrix, or the bilinear model. In general, matrix decomposition is not unique, since inserting a product of an arbitrary invertible matrix and its inverse in between two matrix factors preserves their product. Note also that matrix decomposition can be unique only if one imposes additional problem-specific structural properties including orthogonality, Vandermonde, Toeplitz, constant modulus or finite-alphabet constraints. In contrast to the case of matrices, trilinear model or trilinear decomposition has a distinctive and attractive feature: It is often unique [13]. The uniqueness of trilinear decomposition is of great practical significance, which is crucial in many applications such as psychometrics and chemistry. Thus, trilinear decomposition is naturally related to linear algebra for multi-way data. In the signal processing field, trilinear decomposition can be regarded as a generalization of ESPRIT and joint approximate diagonalization ideas [14, 15], and has been widely used in blind signal detection [16–18] and parameter estimation [19–22].

Parameter identifiability of MIMO radar [7] is defined as the maximum number of targets that can be uniquely identified by the radar. The identifiability results (based on ULA) have been shown that the waveform diversity afforded by MIMO radar enables the significantly improved parameter identifiability over its phased-array counterpart [2, 7]. In this paper, we give the identifiability results with reference to different transmit/receive array manifolds. We construct the trilinear model to deal with the problem of angle estimation for

MIMO radar, and then derive a trilinear decomposition-based angle estimation algorithm. Simulation results illustrate the merits of our proposed algorithm and its better angle estimation performance than ESPRIT. We also present numerical results for different array antenna manifolds and a variety of data lengths.

The rest of this paper is organized as follows. Section 2 develops data model. Section 3 and Section 4 are devoted to the algorithmic presentation, identifiability results and angle estimation. Section 5 offers simulation results, while Section 6 summarizes our conclusions.

Notation: $(.)^*$, $(.)^T$, $(.)^H$, $(.)^\dagger$ and $\|\;\|_F$ denote the complex conjugation, transpose, conjugate-transpose, pseudo-inverse operations and Forbenius norm, respectively. $\mathbf{I}_P$ is a $P \times P$ identity matrix; $\circ$ is Khatri-Rao product; $\otimes$ is the Kronecker product. $\mathbf{0}_I$ is an $I \times 1$ vector of all zeros. $D_m(.)$ is to extract the mth row of its matrix argument and construct a diagonal matrix out of it. angle (.) returns the phase angles for each element of complex array.

2. DATA MODEL

Consider a bistatic MIMO radar system, which includes an M-element transmit array and an N-element receiver array. We assume that there are K uncorrelated targets located at the same range, and the output of the matched filters at the receiver can be expressed as [10],

$$\mathbf{X} = [\mathbf{a}_r(\boldsymbol{\varphi}_1) \otimes \mathbf{a}_t(\boldsymbol{\theta}_1), \mathbf{a}_r(\boldsymbol{\varphi}_2) \otimes \mathbf{a}_t(\boldsymbol{\theta}_2), \ldots, \mathbf{a}_r(\boldsymbol{\varphi}_K) \otimes \mathbf{a}_t(\boldsymbol{\theta}_K)]\mathbf{B}^T \quad (1)$$

where $\boldsymbol{\theta}_k = (\theta'_k, \theta''_k)$, $\boldsymbol{\varphi}_k = (\phi'_k, \phi''_k)$ are the transmit elevation-azimuth angles and receive elevation-azimuth angles of the kth target with respect to the transmit array normal and the receive array normal, respectively; $\mathbf{B} \in \mathbb{C}^{L\times K}$ consists of the phases and amplitudes of the K sources for L samples, in which phase is caused by Doppler frequency, amplitude is influenced mainly by the reflection coefficients, transmit/receive gain and path losses, etc; $\mathbf{a}_r(\boldsymbol{\varphi}_k) \otimes \mathbf{a}_t(\boldsymbol{\theta}_k)$ is the Kronecker product of the transmit and the receive steering vectors for the kth target. The signal model in (1) can be expressed as

$$\mathbf{X} = [\mathbf{A}_T \circ \mathbf{A}_R]\mathbf{B}^T = \begin{bmatrix} \mathbf{X}_1 \\ \mathbf{X}_2 \\ \vdots \\ \mathbf{X}_M \end{bmatrix} = \begin{bmatrix} \mathbf{A}_R D_1(\mathbf{A}_T) \\ \mathbf{A}_R D_2(\mathbf{A}_T) \\ \vdots \\ \mathbf{A}_R D_M(\mathbf{A}_T) \end{bmatrix} \mathbf{B}^T \quad (2)$$

where $\mathbf{A}_T = [\mathbf{a}_t(\boldsymbol{\theta}_1), \mathbf{a}_t(\boldsymbol{\theta}_2), \ldots, \mathbf{a}_t(\boldsymbol{\theta}_K)] \in \mathbb{C}^{M\times K}$ and $\mathbf{A}_R = [\mathbf{a}_r(\boldsymbol{\varphi}_1), \mathbf{a}_r(\boldsymbol{\varphi}_2), ..., \mathbf{a}_r(\boldsymbol{\varphi}_K)] \in \mathbb{C}^{N\times K}$ are the transmit direction matrix and the receive direction matrix, respectively. $\mathbf{A}_T \circ \mathbf{A}_R$ is Khatri-Rao product, $D_m(.)$ is to extract the mth row of its matrix argument and construct a diagonal matrix out of it. Hence, $\mathbf{X}_m$ can be denoted as

$$\mathbf{X}_m = \mathbf{A}_R D_m(\mathbf{A}_T)\mathbf{B}^T, \quad m = 1, \ldots, M \tag{3}$$

In the presence of noise, the signal model becomes $\tilde{\mathbf{X}}_m = \mathbf{A}_R D_m(\mathbf{A}_T)\mathbf{B}^T + \mathbf{V}_m$, $m = 1, \ldots, M$, where $\mathbf{V}_m$ is the received noise corresponding to the mth slice. Eq. (3) is also denoted with trilinear model [13],

$$x_{m,n,l} = \sum\nolimits_{k=1}^{K} \mathbf{A}_t(m,k)\mathbf{A}_r(n,k)\mathbf{B}(l,k),$$
$$m = 1, \ldots, M; \quad n = 1, \ldots, N; \quad l = 1, ..., L \tag{4}$$

where $\mathbf{A}_r(n,k)$ stands for the (n,k) element of the matrix $\mathbf{A}_r$, and similarly for the others.

Notably, $\mathbf{X}_m = \mathbf{A}_R D_m(\mathbf{A}_T)\mathbf{B}^T$, $m = 1, \ldots, M$, can be interpreted as slicing the 3-D data in a series of slices (2-D data) along the spatial direction. The symmetry of the trilinear model in (4) allows two more matrix system rearrangements, in which we have

$$\mathbf{Y}_n = \mathbf{B} D_n(\mathbf{A}_R)\mathbf{A}_T^T, \quad n = 1, \ldots, N \tag{5}$$

$$\mathbf{Z}_l = \mathbf{A}_T D_l(\mathbf{B})\mathbf{A}_R^T, \quad l = 1, \ldots, L \tag{6}$$

3. TRILINEAR DECOMPOSITION AND ITS IDENTIFIABILITY RESULTS

3.1. Algorithmic Presentation

Trilinear Alternating Least Square (TALS) algorithm is the common data detection method for trilinear model [17]. The principle of TALS can be used to fit low rank trilinear models on the basis of noisy observations. The basic idea behind TALS can be briefly shown for three major steps: 1) Each time update one matrix using least squares (LS) conditioned on previously obtained estimates for the remaining matrices; 2) proceed to update the other matrices; 3) repeat until convergence of the LS cost function. In this section, we discuss TALS algorithm in detail as follows. With respect to (2), LS fitting is

$$\min_{\mathbf{A}_T,\mathbf{A}_R,\mathbf{B}} \left\| \mathbf{X} - [\mathbf{A}_T \circ \mathbf{A}_R]\mathbf{B}^T \right\|_F \tag{7}$$

where $\| \, \|_F$ stands for the Frobenius norm, $\tilde{\mathbf{X}}$ is the noisy signal. LS update for $\mathbf{B}$ is

$$\hat{\mathbf{B}}^T = [\hat{\mathbf{H}} \circ \hat{\mathbf{A}}]^+ \tilde{\mathbf{X}} \tag{8}$$

where $\hat{\mathbf{A}}$ and $\hat{\mathbf{H}}$ are previously obtained estimates of $\mathbf{A}$ and $\mathbf{H}$, respectively.

According to the symmetry of the trilinear model, we form the following matrices,

$$\mathbf{Y} = \begin{bmatrix} \mathbf{Y}_1 \\ \mathbf{Y}_2 \\ \vdots \\ \mathbf{Y}_N \end{bmatrix} = [\mathbf{A}_R \circ \mathbf{B}]\mathbf{A}_T^T \tag{9}$$

where $\mathbf{Y}_n$ is shown in Eq. (5). Meanwhile, with respect to (9), LS fitting is

$$\min_{\mathbf{A}_T, \mathbf{A}_R, \mathbf{B}} \left\| \tilde{\mathbf{Y}} - [\mathbf{A}_R \circ \mathbf{B}]\mathbf{A}_T^T \right\|_F \tag{10}$$

where $\tilde{\mathbf{Y}}$ is the noisy signal. LS update for $\hat{\mathbf{A}}_T$ is

$$\hat{\mathbf{A}}_T^T = [\mathbf{A}_R \circ \mathbf{B}]^+ \tilde{\mathbf{Y}} \tag{11}$$

Similarly, according to (6), we obtain

$$\mathbf{Z} = \begin{bmatrix} \mathbf{Z}_1 \\ \mathbf{Z}_2 \\ \vdots \\ \mathbf{Z}_L \end{bmatrix} = [\mathbf{B} \circ \mathbf{A}_T]\mathbf{A}_R^T \tag{12}$$

LS fitting is

$$\min_{\mathbf{A}_T, \mathbf{A}_R, \mathbf{B}} \left\| \tilde{\mathbf{Z}} - [\mathbf{B} \circ \mathbf{A}_T]\mathbf{A}_R^T \right\|_F \tag{13}$$

where $\tilde{\mathbf{Z}}$ is the noisy signal. LS update for $\hat{\mathbf{A}}_T$ is

$$\hat{\mathbf{A}}_R^T = [\mathbf{B} \circ \mathbf{A}_T]^+ \tilde{\mathbf{Z}} \tag{14}$$

According to (8), (11) and (14), matrices $\mathbf{B}$, $\mathbf{A}_T$ and $\mathbf{A}_R$ are updated with conditioned least squares, respectively. All the matrix updates will stop until convergence. For zero-mean white Gaussian noise, TALS yields rnaximum likelihood (ML) estimates [23]. Under mild regularity conditions, ML is asymptotically unbiased and asymptotically achieves the Cramér-Rao bound (CRB). While TALS algorithm is quite easy to process and guaranteed to converge, its major shortcomings lies on the occasional slowness of the convergence steps [23]. TALS algorithm can be initialized randomly, or initialized by eigen-decomposition to accelerate convergence. To overcome the weakness of TALS, the COMFAC algorithm [24] is hereby adopted, which essentially utilizes a fast implementation of TALS, and speeds up the LS fitting for trilinear decomposition.

3.2. Identifiability Results

Theorem 1 [25]: $\mathbf{X}_m = \mathbf{A}_R D_m(\mathbf{A}_T)\mathbf{B}^T$, $m = 1, \dots, M$, where $\mathbf{A}_T \in \mathbb{C}^{M\times K}$, $\mathbf{A}_R \in \mathbb{C}^{N\times K}$ and $\mathbf{B} \in \mathbb{C}^{L\times K}$, when matrices $\mathbf{A}_T$, $\mathbf{A}_R$ and $\mathbf{B}$ are full k-rank [17], if the parameter identifiability satisfies

$$\min(M, K) + \min(N, K) + \min(L, K) \geq 2(K + 1) \tag{15}$$

then $\mathbf{A}_T$, $\mathbf{A}_R$ and $\mathbf{B}$ and are unique up to permutation and scaling of columns.

Notably, if the receive array is a ULA, $\mathbf{A}_R$ should be a Vandermonde matrix, and hence, the discussion for identifiability should be

$$\min(N + \min(M, K), 2K) + \min(L, K) \geq 2(K + 1) \tag{16}$$

When the transmit array is a ULA, $\mathbf{A}_T$ has been with Vandermonde characteristic, the identifiability results yields

$$\min(N, K) + \min(M + \min(L, K), 2K) \geq 2(K + 1) \tag{17}$$

If the transmit array and receive array are both ULAs, matrices of $\mathbf{A}_T$ and $\mathbf{A}_R$ should be with Vandermonde structure, hence, the identifiability condition should be

$$M + N + \min(L, K) \geq 2K + 2 \tag{18}$$

Generally we have $L \geq K$, and then Eq. (18) becomes $M + N \geq K + 2$. The maximal number of targets which our algorithm can detect $K_{\max} = M + N - 2$ or $K \leq M + N - 2$.

Suppose that $K \geq L$, identifiability condition becomes $M + N + L \geq 2K + 2$, in that case our algorithm can even support small sample.

For the received noisy signal, we use trilinear decomposition to obtain the estimated matrices, in which we have $\hat{\mathbf{A}}_T = \mathbf{A}_T\mathbf{\Pi}\mathbf{\Delta}_1 + \mathbf{N}_1$, $\hat{\mathbf{A}}_R = \mathbf{A}_R\mathbf{\Pi}\mathbf{\Delta}_2 + \mathbf{N}_2$, $\hat{\mathbf{B}} = \mathbf{B}\mathbf{\Pi}\mathbf{\Delta}_3 + \mathbf{N}_3$, where $\mathbf{\Pi}$ is a permutation matrix, $\mathbf{\Delta}_1$, $\mathbf{\Delta}_2$, $\mathbf{\Delta}_3$ are diagonal scaling matrices satisfying $\mathbf{\Delta}_1\mathbf{\Delta}_2\mathbf{\Delta}_3 = \mathbf{I}_K$, $\mathbf{N}_1$, $\mathbf{N}_2$ and $\mathbf{N}_3$ are noise matrices. Within trilinear decomposition, permutation ambiguity and scale ambiguity are inherent. Notably, the scale ambiguity can be resolved by means of normalization.

4. ANGLE ESTIMATION

We firstly use trilinear decomposition to attain the direction matrix, and then obtain the estimates for angles according to LS principle. Different array conditions are considered in this section.

4.1. Uniform Linear Array (ULA)

We consider that the receive array is a ULA with half-wavelength antenna spacing, for which only one-dimension angle can be estimated. Define $\boldsymbol{\varphi}_k = (\phi_k', \phi_k'')$, where ϕ_k', ϕ_k'' are the receive elevation angle and the azimuth angle of the kth target, respectively; assume $\phi_k' = 90°$ in the ULA. The receive array steer vector for $\boldsymbol{\varphi}_k$ is given by $\mathbf{a}_r(\boldsymbol{\varphi}_k) = [1, e^{-j\pi \sin\phi_k''}, \ldots, e^{-j\pi(N-1)\sin\phi_k''}]^T$, from which we get

$$\mathbf{h} = -angle(\mathbf{a}_r(\boldsymbol{\varphi}_k)) \tag{19}$$

After this operation, Eq. (19) becomes $\mathbf{h} = [0, \pi\sin\phi_k'', ..., \pi(N-1)\sin\phi_k'']^T$, then LS principle is adopted to estimate $\sin\phi_k''$.

In the following steps, the estimated receive array steer vector $\hat{\mathbf{a}}_r(\boldsymbol{\varphi}_i)$ (the ith column of the estimated matrix $\hat{\mathbf{A}}_R$) is processed through normalization, which also resolves the scale ambiguity. Moreover, the normalized sequence is processed to attain $\hat{\mathbf{h}}$ with respect to Eq. (19). Finally, LS principle is adopted to obtain the estimated value of $\sin\phi_i''$.

We have LS fitting given by

$$\mathbf{P}_1\mathbf{c} = \hat{\mathbf{h}}$$

where

$$\mathbf{P}_1 = \begin{bmatrix} 1 & 0 \\ 1 & \pi \\ \vdots & \vdots \\ 1 & \pi(N-1) \end{bmatrix} \tag{20}$$

$\mathbf{c} = \begin{bmatrix} f_0 \\ f_i \end{bmatrix}$, in which f_i represents the estimated value of $\sin\phi_i''$.

Obviously, the LS solution for $\mathbf{c}$ is shown as

$$\begin{bmatrix} \hat{f}_0 \\ \hat{f}_i \end{bmatrix} = (\mathbf{P}_1^T\mathbf{P}_1)^{-1}\mathbf{P}_1^T\hat{\mathbf{h}}$$

Correspondingly, the receive angle ϕ_i'' can be estimated via

$$\phi_i'' = \sin^{-1}\left(\hat{f}_i\right) \tag{21}$$

Provided that the transmit array is also a ULA, the matrices $\mathbf{A}_T$ and $\mathbf{A}_R$ should be also with Vandermonde characteristic, and hence, we can use the same method to estimate transmit angle.

4.2. Uniform Circular Array (UCA)

We also consider that a UCA is adopted by the receive array, then the receive array steer vector, for which $\boldsymbol{\varphi}_k = (\phi'_k, \phi''_k)$, can be written as

$$\mathbf{a}_r(\boldsymbol{\varphi}_k) = \begin{bmatrix} \exp\left(j2\pi R\sin(\phi'_k)\cos\left(\phi''_k - 0\right)/\lambda\right) \\ \exp\left(j2\pi R\sin(\phi'_k)\cos\left(\phi''_k - \frac{2\pi}{N}\right)/\lambda\right) \\ \vdots \\ \exp\left(j2\pi R\sin(\phi'_k)\cos\left(\phi''_k - \frac{2\pi(N-1)}{N}\right)/\lambda\right) \end{bmatrix} \tag{22}$$

where R is the radius of UCA. With respect to (22), we firstly divide each column by the first element, then remove the first element to get an new vector $\mathbf{a}_1$, and finally obtain angle $(\mathbf{a}_1)$, which is shown

$$\begin{bmatrix} \xi\sin\phi'_k\cos\phi''_k\left(\cos\frac{2\pi}{N}-1\right) + \xi\sin\phi'_k\sin\phi''_k\sin\frac{2\pi}{N} \\ \xi\sin\phi'_k\cos\phi''_k\left(\cos\frac{2\times 2\pi}{N}-1\right) + \xi\sin\phi'_k\sin\phi''_k\sin\frac{2\times 2\pi}{N} \\ \vdots \\ \xi\sin\phi'_k\cos\phi''_k\left(\cos\frac{(N-1)2\pi}{N}-1\right) + \xi\sin\phi'_k\sin\phi''_k\sin\frac{(N-1)2\pi}{N} \end{bmatrix} \tag{23}$$

where $\xi = 2\pi R/\lambda$. In Eq. (23), ith element is divided by $(\cos\frac{2\pi i}{N} - 1)$, $i = 1, \ldots, M-1$, then we get

$$\mathbf{g} = \begin{bmatrix} c_0 + c_1\sin\frac{2\pi}{N}/\left(\cos\frac{2\pi}{N}-1\right) \\ c_0 + c_1\sin\frac{2\times 2\pi}{N}/\left(\cos\frac{2\times 2\pi}{N}-1\right) \\ \vdots \\ c_0 + c_1\sin\frac{(N-1)2\pi}{N}/\left(\cos\frac{(N-1)2\pi}{N}-1\right) \end{bmatrix} \tag{24}$$

where $c_0 = \xi\sin\phi'_k\cos\phi''_k$, $c_1 = \xi\sin\phi'_k\sin\phi''_k$. We also use LS principle to estimate DOA. Throughout trilinear decomposition, the estimated direction vector $\hat{\mathbf{a}}_r(\boldsymbol{\varphi}_k)$ is attainable. The estimated direction vector is processed like mentioned above to get $\hat{\mathbf{g}}$. LS fitting is hereby referred as

$$\mathbf{P}_2\begin{bmatrix} c_0 \\ c_1 \end{bmatrix} = \hat{\mathbf{g}}$$

where

$$\mathbf{P}_2 = \begin{bmatrix} 1 & \sin\frac{2\pi}{N}/\left(\cos\frac{2\pi}{N}-1\right) \\ 1 & \sin\frac{2\times 2\pi}{N}/\left(\cos\frac{2\times 2\pi}{N}-1\right) \\ \vdots & \vdots \\ 1 & \sin\frac{(N-1)2\pi}{N}/\left(\cos\frac{(N-1)2\pi}{N}-1\right) \end{bmatrix} \tag{25}$$

Similarly, LS principle for the estimate of $\begin{bmatrix} c_0 \\ c_1 \end{bmatrix}$ is shown

$$\begin{bmatrix} \hat{c}_0 \\ \hat{c}_1 \end{bmatrix} = \left(\mathbf{P}_2^T \mathbf{P}_2\right)^{-1} \mathbf{P}_2^T \hat{\mathbf{g}} \tag{26}$$

Furthermore, DOA estimation can be given by

$$\phi'_k = \sin^{-1}\left(\sqrt{\hat{c}_0^2 + \hat{c}_1^2}/\xi\right) \tag{27}$$

$$\phi''_k = \tan^{-1}\left(\hat{c}_1/\hat{c}_0\right) \tag{28}$$

4.3. L-shaped Array

We consider an L-shaped array with sensors at M different locations as shown in Fig. 1. A uniform linear array (ULA) containing M_1 elements is located in Y-axis, and the other ULA containing M_2 $(M_2 + M_1 = M + 1)$ elements is located in X-axis. Antenna spacing is half-wavelength. The receive array steer vector for $\boldsymbol{\varphi}_k = (\phi'_k, \phi''_k)$ is divided into two parts, which is shown as follows

$$\mathbf{a}_x(\boldsymbol{\varphi}_k) = \begin{bmatrix} 1 & e^{-j\pi\cos\phi'_k \sin\phi''_k} & \dots & e^{-j\pi(M_2-1)\cos\phi'_k \sin\phi''_k} \end{bmatrix}^T \tag{29a}$$

$$\mathbf{a}_y(\boldsymbol{\varphi}_k) = \begin{bmatrix} 1 & e^{-j\pi\sin\phi'_k \sin\phi''_k} & \dots & e^{-j\pi(M_1-1)\sin\phi'_k \sin\phi''_k} \end{bmatrix}^T \tag{29b}$$

According to (29a) and (29b), we obtain

$$\mathbf{g}_x = -angle\left(\mathbf{a}_x(\boldsymbol{\varphi}_k)\right) \tag{30a}$$

$$\mathbf{g}_y = -angle\left(\mathbf{a}_y(\boldsymbol{\varphi}_k)\right) \tag{30b}$$

Define $m_x = \cos\phi'_k \sin\phi''$, $n_y = \sin\phi'_k \sin\phi''_k$, then Eqs. (30a) and (30b) becomes

$$\begin{aligned} \mathbf{g}_x &= [0, \pi m_x, \dots, \pi(M_2 - 1)m_x]^T \\ \mathbf{g}_y &= [0, \pi n_y, \dots, \pi(M_1 - 1)n_y]^T. \end{aligned}$$

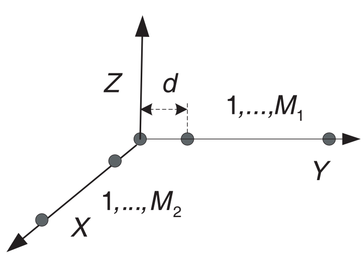

Figure 1. The structure of an L-shaped array.

The estimated receive array steer vector $\hat{\mathbf{a}}_r(\boldsymbol{\varphi}_i)$ (the ith column of the estimated matrix $\hat{\mathbf{A}}_R$) is processed through normalization, and divided two parts like (29a) and (29b), and then normalized sequences are processed to attain $\mathbf{g}_x$ and $\mathbf{g}_y$ according to Eqs. (30a) and (30b), respectively. LS principle is used to obtain the estimated value of $\cos\phi'_k \sin\phi''$ and $\sin\phi'_k \sin\phi''_k$.

Similarly, LS fitting is denoted as

$$\mathbf{P}_1\mathbf{c} = \mathbf{g}_x$$

where $\mathbf{P}_1$ is shown in Eq. (20),

$$\mathbf{c}_1 = \begin{bmatrix} m_0 \\ m_x \end{bmatrix}$$

The estimate for $\mathbf{c}_1$ adopted by LS principle is written as

$$\begin{bmatrix} \hat{m}_0 \\ \hat{m}_x \end{bmatrix} = (\mathbf{P}_1^T\mathbf{P}_1)^{-1}\mathbf{P}_1^T\hat{\mathbf{g}}_1 \tag{31}$$

Meanwhile, we have LS fitting for $\mathbf{g}_y$

$$\mathbf{P}_1\mathbf{c}_2 = \mathbf{g}_y$$

where

$$\mathbf{c}_2 = \begin{bmatrix} n_0 \\ n_y \end{bmatrix}$$

Then the estimate for $\mathbf{c}_2$ becomes

$$\begin{bmatrix} \hat{n}_0 \\ \hat{n}_y \end{bmatrix} = (\mathbf{P}_1^T\mathbf{P}_1)^{-1}\mathbf{P}_1^T\hat{\mathbf{g}}_2 \tag{32}$$

DOA estimation is finally shown as

$$\hat{\phi}''_{k_i} = \sin^{-1}\left(\sqrt{\hat{m}_x^2 + \hat{n}_y^2}\right) \tag{33}$$

$$\hat{\varphi}'_k = \tan^{-1}\left(\hat{n}_y/\hat{m}_x\right) \tag{34}$$

In sum, we have deducted trilinear decomposition-based blind angle estimation for MIMO radar and shown the detailed steps as before. Our algorithm firstly applies trilinear decomposition to obtain the estimated direction matrices, then estimate angles correspondingly with respect to LS principle.

Computational cost can be evaluated as follows. In our algorithm, the complexity of each TALS iteration is $O(K^3 + MNLK)$, and the number of iterations depends on the three way data to be decomposed. In contrast, ESPRIT normally requires $O(LM^2N^2 + M^3N^3 + K^3)$.

5. SIMULATION RESULTS

The received noisy signal is $\tilde{\mathbf{X}}_m = \mathbf{A}_R D_m(\mathbf{A}_T)\mathbf{B}^T + \mathbf{W}_m$, $m = 1, \ldots, M$, where $\mathbf{W}_m$ is the additive Gaussian white noise (AWGN) matrix. We define SNR

$$\mathrm{SNR} = 10\log_{10} \frac{\sum_{m=1}^{M} \left\|\mathbf{A}_R D_m(\mathbf{A}_T)\mathbf{B}^T\right\|_F^2}{\sum_{m=1}^{M} \left\|\mathbf{W}_m\right\|_F^2} dB \tag{35}$$

We present Monte Carlo simulations to assess the angle estimation performance of the proposed algorithm. The number of Monte Carlo trials is 500. Note that: L is the number of snapshots.

Define root mean squared error (RMSE) as $RMSE = \sqrt{\frac{1}{500}\sum_{m=1}^{500} (\hat{\theta}'^{,m} - \theta')^2 + (\hat{\theta}''^{,m} - \theta'')^2}$, where $\hat{\theta}'^{,m}$, $\hat{\theta}''^{,m}$ are the estimated transmit elevation-azimuth angles of the mth Monte Carlo trial, respectively. RMSE of the receive angles can also be defined as above.

Firstly, we consider that transmit array and receive array are both ULAs in a bistatic MIMO radar. $M = 8$ and $N = 6$ is used in the simulations. Three noncoherent sources are assumed to be located at angles $(\theta_1'', \phi_1'') = (10°, 15°)$, $(\theta_2'', \phi_2'') = (20°, 25°)$ and $(\theta_3'', \phi_3'') = (30°, 35°)$, respectively. We firstly investigate the convergence performance of our proposed algorithm in this simulation. The sum of squared residuals (SSR) in the trilinear fitting is defined as $SSR = \sum_{m,n,l} [\tilde{x}_{m,n,l} - \sum_{k=1}^{K} \mathbf{A}_t(m,k)\mathbf{A}_r(n,k)\mathbf{B}(l,k)]^2$, where $\tilde{x}_{n,k,i}$ is the noisy data. Define $DSSR = SSR_i - SSR_0$, where SSR_i is the SSR of the ith iteration, SSR_0 is the SSR in the convergence condition. Fig. 2 presents the algorithmic convergence performance of

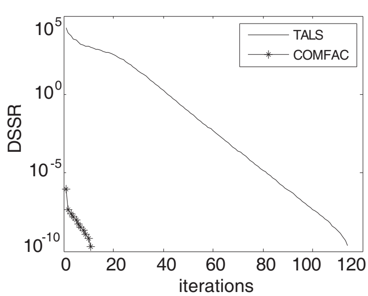

Figure 2. The algorithm convergence performance.

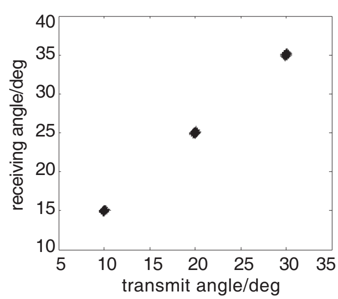

Figure 3. Angle estimation results of proposed algorithm for all three targets with both ULAs.

our algorithm with $L = 50$ and SNR $= 20$ dB. From Fig. 2, COMFAC algorithm has faster convergence than TALS.

Figure 3 shows angle estimation RMSE results of our proposed algorithm. The algorithmic simulation have been verified over 100 Monte Carlo trials in condition of SNR $= 8$ dB. From Fig. 3, we find that our algorithm works well. Then we present the algorithmic comparison (in contrast to ESPRIT and multi-invariance MUSIC algorithm [26]) with $L = 40$. Fig. 4 depicts RMSE of estimation for three targets under different SNR. From Fig. 4, we find that our algorithm has better angle estimation than ESPRIT algorithm [10], and our algorithm has slightly better angle estimation than multi-

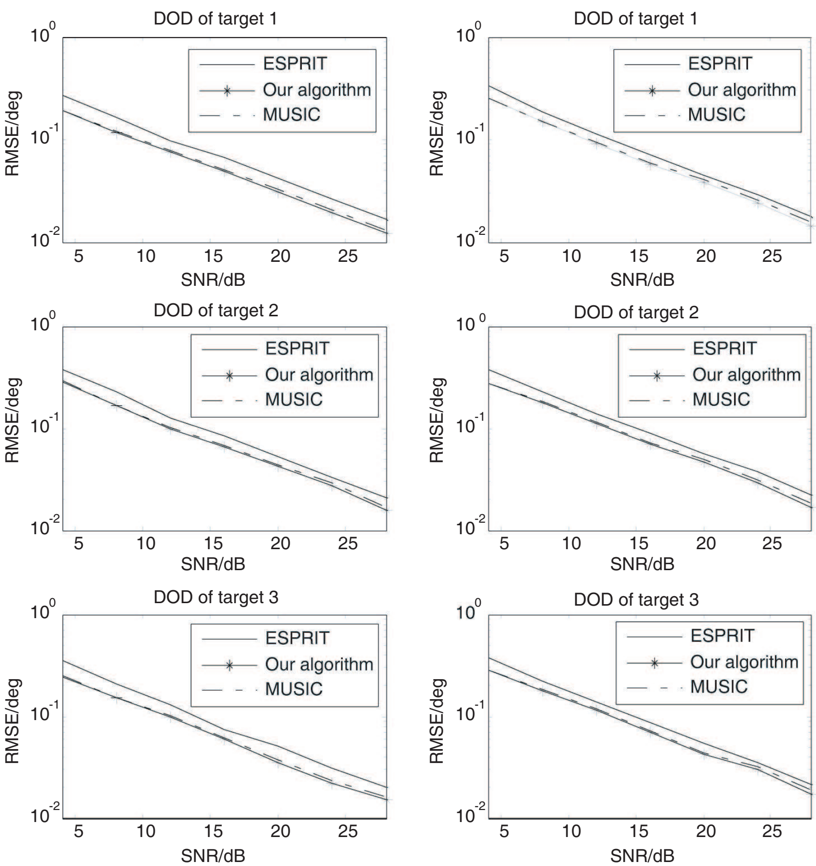

Figure 4. RMSE of estimation for two targets with different SNR (both ULAs, and $L = 40$).

invariance MUSIC algorithm. TALS, which is used for trilinear decomposition in our algorithm, can be optimal for additive i.i.d. Gaussian noise [23], and hence, our algorithm has improved angle estimation performance than ESPRIT algorithm.

Figure 5 presents angle estimation performance of our algorithm with different numerical values of L. It is indicated in Fig. 5 that with the multiplies of L increasing, angle estimation performance via our proposed method is improving. Fig. 5 also shows small sample results: $L = 5$. It is clear that our algorithm can even perform well for a quite small sampling sizes.

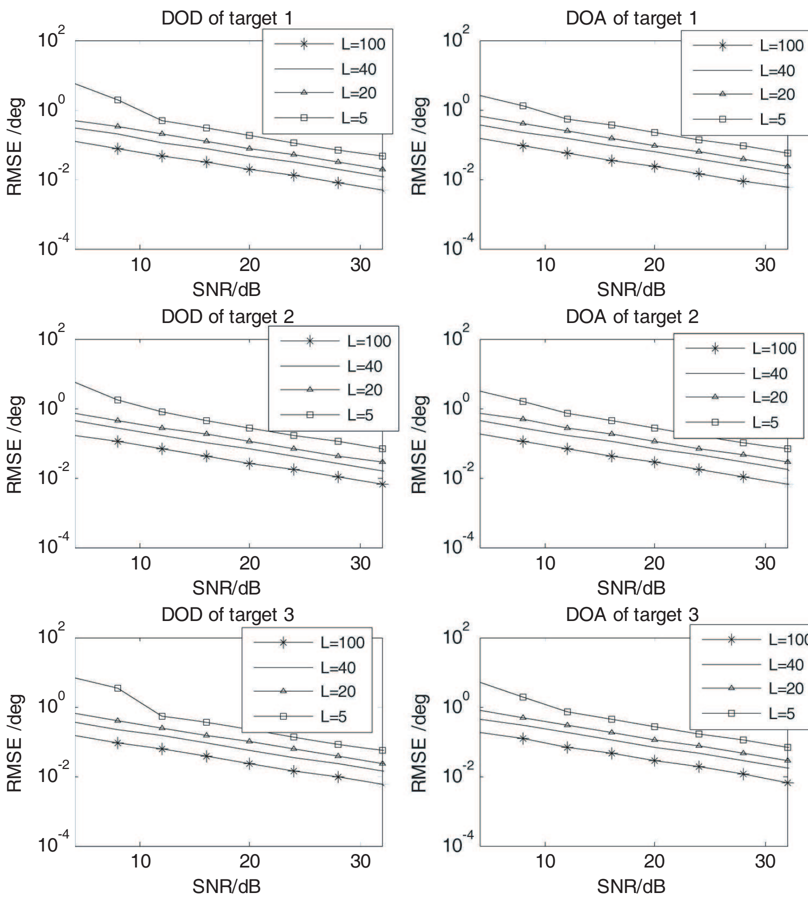

Figure 5. Angle estimation for three targets with different L (both ULAs).

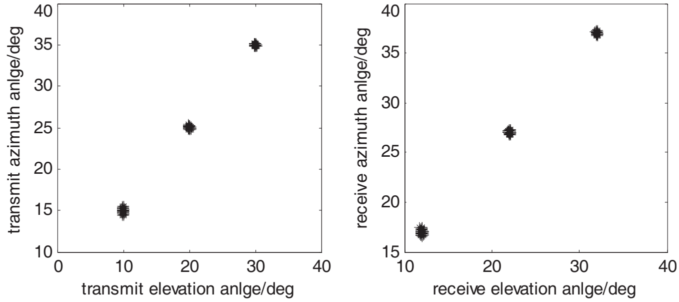

Figure 6. Angle estimation results of proposed algorithm for all three targets with both UCAs (SNR $= 20\,\text{dB}$).

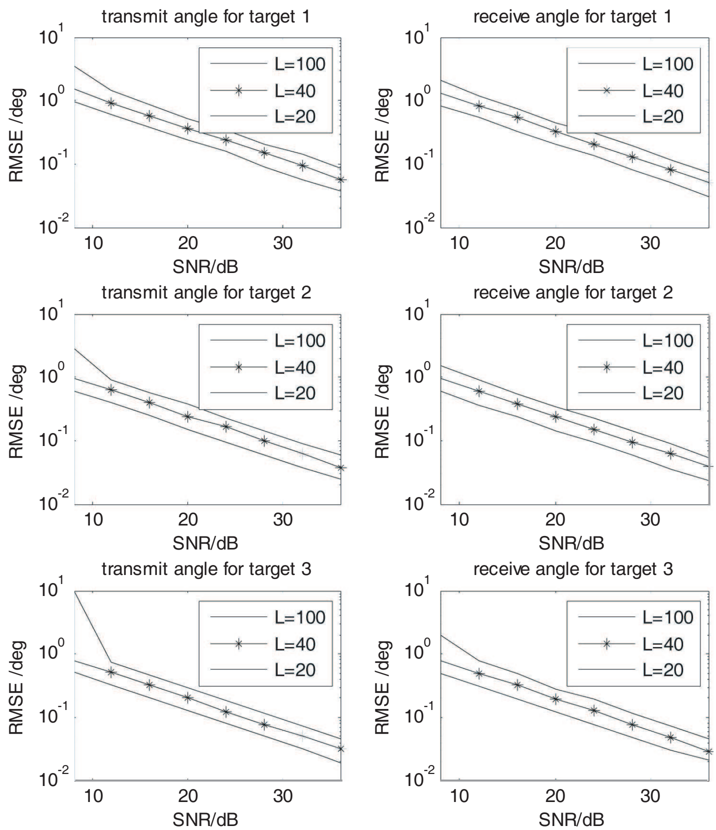

Figure 7. Angle estimation for three targets with different L (both UCAs).

Then we consider that transmit array and receive array are both uniform circular arrays (UCA) in MIMO radar. 8-element transmit array and 8-element receive array are used in the simulation, both of which R is half-wavelength. Three noncoherent targets are hereby assumed to be located at angles $(\theta_1', \theta_1'', \phi_1', \phi_1'') = (10°, 15°, 12°, 17°)$, $(\theta_2', \theta_2'', \phi_2', \phi_2'') = (20°, 25°, 22°, 27°)$, $(\theta_3', \theta_3'', \phi_3', \phi_3'') = (30°, 35°, 32°, 37°)$, respectively. Fig. 6 shows angle estimation RMSE results of the proposed algorithm for all three targets over 100 Monte Carlo simulations with SNR = 20 dB. From Fig. 6, we find that our algorithm works well in condition of both UCAs. Moreover, Fig. 7 presents RMSE of estimation for three targets under different L. From Fig. 7, it is also noted that the angle estimation performance of our proposed algorithm is improved with L increasing.

Furthermore, both L-shaped arrays have been adopted for transmit/receive array of MIMO-radar in the simulations followed by. 9-element transmit array and 9-element receive array have been used in the simulation. We assume that the three noncoherent targets have been located at angles $(\theta_1', \theta_1'', \phi_1', \phi_1'') = (10°, 15°, 10°, 15°)$, $(\theta_2', \theta_2'', \phi_2', \phi_2'') = (20°, 25°, 20°, 25°)$, $(\theta_3', \theta_3'', \phi_3', \phi_3'') = (30°, 35°, 30°, 35°)$, respectively. Fig. 8 presents angle estimation results of the proposed algorithm for all three targets over 100 Monte Carlo simulations with SNR = 20 dB. From Figs. 8–9, we find that our algorithm has meritorious performance with both L-shaped arrays. Angle estimation performance of our algorithm with different values of L is proposed in Fig. 9. Clearly, it is indicated in Fig. 9 that similar improvements for angle estimation performance of our algorithm comes out with L increasing.

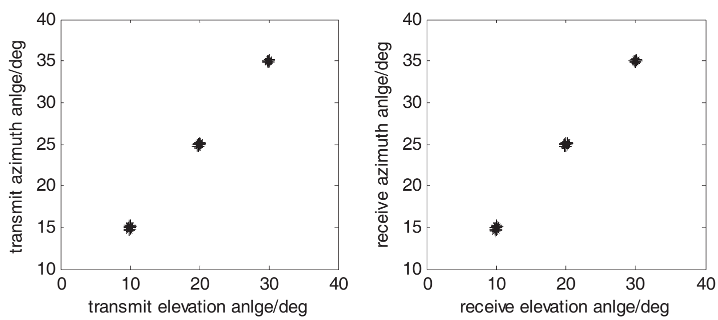

Figure 8. Angle estimation results of the proposed algorithm for all three targets with both L-shaped arrays (SNR = 20 dB).

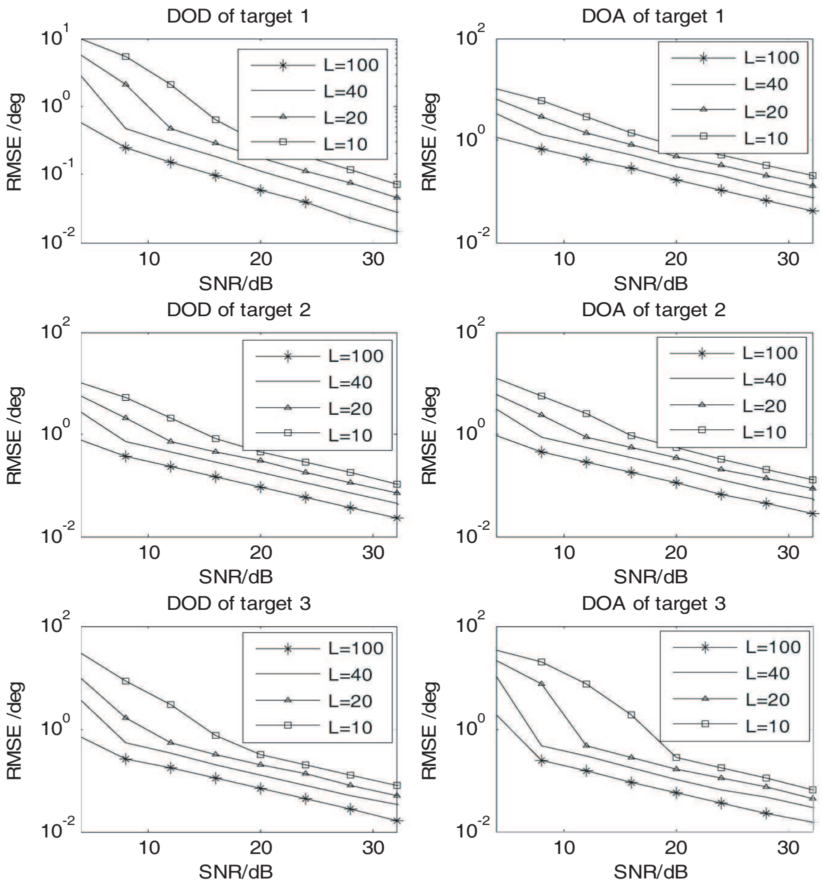

Figure 9. Angle estimation for three targets with different L (both L-shaped arrays).

6. CONCLUSION

In this paper, we have expanded the application of trilinear model, and derived a blind angle estimation algorithm for MIMO radar. Deductions for the proposed algorithm, as well as identifiability results, have been presented with reference to several transmit/receive array manifolds, independently. The usefulness of our method has been verified that it has better performance of angle estimation than that of ESPRIT, and can be compatible for different array conditions.

ACKNOWLEDGMENT

This work is supported by China NSF Grants (60801052), Jiangsu NSF Grants (BK2007192), Aeronautical Science Foundation of China (2008ZC52026) and Ph.D. programs foundation of China's ministry of education (200802871056). The authors wish to thank the anonymous reviewers for their valuable suggestions on improving this paper.

REFERENCES

1. Fishler, E., A. Haimovich, R. S. Blum, L. J. Cimini, D. Chizhik, and R. A. Valenzuela, "MIMO radar: An idea whose time has come," *Proc. IEEE Radar Conf.*, 71–78, Apr. 2004.
2. Li, J. and P. Stoica, "MIMO radar — Diversity means superiority," *Proc. 14th Adaptive Sensor Array Process. Workshop (ASAP'06, Invited)*, MIT Lincoln Laboratory, Lexington, MA, Jun. 2006.
3. Fishler, E., A. Haimovich, R. S. Blum, et al., "Spatial diversity in radars models and detection performance," *IEEE Trans. Signal Process.*, Vol. 54, No. 3, 823–838, 2006.
4. Fuhrmann, D. R. and G. S. Antonio, "Transmit beamforming for MIMO radar systems using partial signal correlation," *Proc. 38th Asilomar Conf. on Signals, Systems and Comput.*, Vol. 1, 295–299, Nov. 2004.
5. Xu, L., J. Li, and P. Stoica, "Adaptive techniques for MIMO radar," *Proc. 4th Workshop on Sensor Array and Multichannel Signal Process.*, 258–262, Jul. 2006.
6. Robey, F. C., S. Coutts, D. D. Weikle, J. C. McHarg, and K. Cuomo, "MIMO radar theory and experimental results," *Proc. 38th Asilomar Conf. Signals, Systems and Computers*, Vol. 1, 300–304, Nov. 2004.
7. Li, J., P. Stoica, L. Xu, and W. Roberts, "On parameter identifiability of MIMO radar," *IEEE Signal Process. Lett.*, Vol. 14, No. 12, 968–971, Dec. 2007.
8. Bekkerman, I. and J. Tabrikian, "Target detection and localization using MIMO radars and sonars," *IEEE Trans. Signal Process.*, Vol. 5, No. 10, 3873–3883, Oct. 2006.
9. Xu, L., J. Li, and P. Stoica, "Target detection and parameter estimation for MIMO radar systems," *IEEE Trans. Aeros. & Electro. Syst.*, Vol. 44, No. 3, 927–939, Jul. 2008.
10. Duofang, C., C. Baixiao, and Q. Guodong, "Angle estimation

using ESPRIT in MIMO radar," *Electron. Lett.*, Vol. 44, No. 12, 770–771, 2008.
11. Jinli, C., G. Hong, and S. Weimin, "Angle estimation using ESPRIT without pairing in MIMO radar," *Electron. Lett.*, Vol. 44, No. 24, 1422–1423, 2008.
12. Jin, M., G. Liao, and J. Li, "Joint DOD and DOA estimation for bistatic MIMO radarr," *Signal Process.*, Vol. 89, No. 2, 244–251, 2009.
13. Kruskal, J. B., "Three-way arrays: Rank and uniqueness of trilinear decompositions, with application to arithmetic complexity and statistics," *Linear Algebra Applicat.*, Vol. 18, 95–138, 1977.
14. De Lathauwer, L., B. De Moor, and J. Vandewalle, "Computation of the canonical decomposition by means of a simultaneous generalized schur decompositition," *SIAM J. Matrix Anal. Appl.*, Vol. 26, No. 2, 295–327, 2004.
15. De Lathauwer, L., "A link between the canonical decomposition in multilinear algebra and simultaneous matrix diagonalization," *SIAM J. Matrix Anal. Appl.*, Vol. 28, No. 3, 642–666, 2006.
16. Zhang, X., X. Gao, and Z. Wang, "Blind paralind multiuser detection for smart antenna CDMA system over multipath fading channel," *Progress In Electromagnetics Research*, PIER 89, 23–38, 2009.
17. Sidiropoulos, N. D., G. B. Giannakis, and R. Bro, "Blind PARAFAC receivers for DS-CDMA systems," *IEEE Trans. Signal Process.*, Vol. 48, No. 3, 810–823, Mar. 2000.
18. Zhang, X. and D. Xu, "Blind PARAFAC signal detection for polarization sensitive array," *Eurasip J. Adv. Signal Process.*, Vol. 2007, 1–7, Article ID 12025, 2007.
19. Sidiropoulos, N. D., R. Bro, and G. B. Giannakis, "Parallel factor analysis in sensor array processing,"*IEEE Trans. Signal Process.*, Vol. 48, No. 8, 2377–2388, Aug. 2000.
20. Zhang, X., Y. Shi, and D. Xu, "Novel blind joint direction of arrival and polarization estimation for polarization-sensitive uniform circular array," *Progress In Electromagnetics Research*, PIER 86, 19–37, 2008.
21. Liu, X., N. D. Sidiropoulos, and A. Swami, "Blind high-resolution localization and tracking of multiple frequency hopped signals," *IEEE Trans. Signal Process.*, Vol. 50, No. 4, 889–901, Apr. 2002.
22. Zhang, X. and D. Xu, "Novel joint time delay and frequency estimation method," *IET Radar, Sonar & Navigation*, Vol. 3,

No. 2, 186–194, 2009.

23. Vorobyov, S. A., Y. Rong, and N. D. Sidiropoulos, "Robust iterative fitting of multilinear models," *IEEE Trans. Signal Process.*, Vol. 53, No. 8, 2678–2689, Aug. 2005.
24. Bro, R., N. D. Sidiropoulos, and G. B. Giannakis, "A fast least squares algorithm for separating trilinear mixtures," *Proc. Inter. Workshop ICA and BSS*, 289–294, France, Jan. 1999.
25. Sidiropoulos, N. D. and X. Liu, "Identifiability results for blind beamforming in incoherent multipath with small delay spread," *IEEE Trans. Signal Process.*, Vol. 49, No. 1, 228–236, Jan. 2001.
26. Swindlehurst, A. L., P. Stoica, and M. Jansson, "Exploiting arrays with multiple invariances using MUSIC and MODE," *IEEE Trans. Signal Process.*, Vol. 49, No. 11, 2511–2521, Nov. 2001.